


# Is There Preclinical and Clinical Value for $^{19}\text{F}$ MRI in Stem Cell Cardiac Regeneration?

Cell Transplantation  
Volume 29: 1–7  
© The Author(s) 2020  
Article reuse guidelines:  
sagepub.com/journals-permissions  
DOI: 10.1177/0963689720954434  
journals.sagepub.com/home/ctj  


Christakis Constantinides<sup>1</sup> 

## Abstract

Cardiovascular regeneration aims to renew damaged or necrotic tissue and to enhance cardiac functional performance. Despite the hope arisen from the introduction and use of stem cells (SCs) as a novel cardiac regenerative approach, to-this-date, clinical trial findings are still ambivalent despite preclinical successes. Concurrently, noninvasive magnetic resonance imaging (MRI) advances have been based on nanotechnological breakthroughs that have (a) allowed fluorinated nanoparticles and ultrasmall iron oxide single-cell labeling, (b) explored imaging detection sensitivity limits (for preclinical/low-field clinical settings), and (c) accomplished cellular tracking *in vivo*. Nevertheless, outcomes have been far from ideal. Herein, the recently developed preclinical and clinical  $^1\text{H}$  and  $^{19}\text{F}$  MRI approaches for direct cardiac SC labeling techniques intended for cellular implantation and their potential for tracking these cells in health and infarcted states are summarized. To this extent, the potential preclinical and clinical values of  $^{19}\text{F}$  MRI and tracking of SCs for cardiac regeneration in myocardial infarction are questioned and challenged.

## Keywords

cardiac regeneration, cardiac stem cells, cell labeling, cell tracking, magnetic resonance imaging

## Introduction

Cardiovascular disease (coronary artery disease, hypertension, and heart failure) is still the primary cause of mortality and morbidity in the Western World. The basic regenerative approaches related to the use of stem cells (SCs) in cardiovascular disease have primarily targeted myocardial infarction (MI)<sup>1–3</sup> and heart failure<sup>4,5</sup>. Critical to SC interventions is a detailed understanding of the onset and progression of MI and the underlying molecular and signaling pathways. A detailed description of the onset/evolution of reperfused MI is summarized herein at the tissue/molecular levels, as originally proposed by Blankensteijn<sup>6</sup>, and enriched with added knowledge from immune research studies<sup>7,8</sup>. Five phases have been proposed to describe the onset and progression of MI, including: (a) Phase I (6 h–2 days post-MI): cardiomyocyte death, (b) Phase II (12–16 h to 3 days post-MI): inflammatory response, (c) Phase III (1–2 weeks post-MI): granulation tissue formation (proliferation), (d) Phase IV (2–3 weeks post-MI): remodeling (proliferation), and (e) Phase V (more than 3 weeks post-MI): maturation.

While extensive cell death is triggered/occurs during Phase I, secondary necrosis ensues during Phase II. Dying cells (with compromised energetic status, channel function, and altered ionic concentrations) release reactive oxygen species, proteolytic enzymes, and intracellular moieties that

serve as “alarmins,” that is, proteins/peptides that activate immune paths and/or other cells that express advanced glycation and toll-like receptors and end by-products that trigger inflammation<sup>7</sup>. The inflammatory response is mediated by the migration of overactive neutrophils and granulocytes in the infarct area that in turn release proinflammatory mediators that promote additional cell death. Monocyte–platelet–monocyte interactions induce specialized pro-resolving lipid mediators, including lipoxins, resolvins, protectins, and maresins, that in conjunction with transforming growth factor and interleukin (IL-10), act as suppressive negative feedback biosignals that limit further neutrophil infiltration and promote anti-inflammatory responses<sup>9,10</sup>. The anti-inflammatory responses are triggered partly via the recruitment of anti-inflammatory macrophages. The removal of dead tissue in conjunction with matrix degradation is mediated via plasmin and metalloproteins (within 1 to 2 days

<sup>1</sup> Chi Biomedical Ltd., Limassol, Cyprus

Submitted: April 9, 2020. Revised: July 5, 2020. Accepted: August 12, 2020

### Corresponding Author:

Christakis Constantinides, Chi Biomedical Ltd., 2 Evryviadou Street, Limassol 4151, Cyprus.

Email: Christakis.Constantinides@gmail.com



post-MI)<sup>6</sup>. Recent evidence has been supportive of the coexistence of proinflammatory (M1) and anti-inflammatory (M2) monocyte phenotypes at the infarct zone<sup>11</sup>.

Phase III (also known as the proliferative phase) demarcates the onset of granulated tissue formation and the scavenging/degradation of necrotic tissue/debris. These effects are mediated by the infiltration of M2 macrophages and lymphocytes that secrete cytokines and growth factors. In turn, these modulate the functions of the resident fibroblasts, fibroblast progenitor cells, cardiac pericytes, and vascular and smooth muscle cells, and lead to the production of myofibroblast-like cells that synthesize structural and extracellular matrix (ECM) proteins (fibrin, tenascin, interstitial collagen I and III, reticulins, and elastins/tropoelastins)<sup>9,10</sup>. This phase is characterized by a dynamic interplay/balance between wall thinning and infarct rupture.

Phase IV is characterized by remodeling or scar formation (proliferation phase). It is followed by the maturation phase V characterized by the reorganization of the structural network (and subsequent fibrosis) owing to changes in the constituent cellular elements, debris, scar, and ECM elements. This phase is characterized by a prominent loss of cellularity, the persistent presence of myofibroblasts, and the completion of the collagen cross-linking process<sup>6</sup>.

This commentary overviews (a) recent SC labeling approaches and their use in cardiac implantation (preclinically and clinically), and (b) <sup>1</sup>H and <sup>19</sup>F MRI attempts for visualization and potential tracking in normal/infarcted states. Potential applications and pathological circumstances wherein <sup>19</sup>F MRI can potentially outperform alternative (current state-of-the-art) methods are outlined.

## Cardiac Stem Cell Therapy

Therapeutic MI treatments with SCs have been studied for more than two decades. Nevertheless, the question on whether these therapies evoke potential functional benefits is still debated. Observed variations documented by the findings of various completed and ongoing clinical trials<sup>1-3,12</sup> that have been/are focusing on mesenchymal SCs, cardiac progenitor cells (CPCs), embryonic stem cells (ESCs), and inducible pluripotent SCs (iPSCs) (Table 1) may be attributed to (among others) the differences in the design and cell preparation parameters, suitable cell type(s), administration route(s), delivery time<sup>13</sup>, and end points<sup>12</sup>. The existing hypotheses for documented SC effects include (a) direct (cardiomyogenesis and vasculogenesis) and (b) indirect (attenuation of inflammatory responses and fibrosis, promotion of angiogenesis, and enhancement of cellular viability via paracrine/other signaling/post-translational modification mechanisms) mechanisms<sup>12,14,15</sup>. Despite the ambivalent clinical outcomes, preclinical successes have been documented in rodents and mammals, as manifested by feasible and safe SC administration, the capacity to change the course of the MI, and improved remodeling and cardiac functional

**Table 1.** Size and Cell Division Characteristics of Prominent Stem Cell Types Used for Cardiac Generation.

Cell type	Indicative cell sizes ( $\mu\text{m}$ )	Doubling time (days)
Mesenchymal stem cells	15–30	$\sim 0.5\text{--}2.5$ <sup>17</sup>
Cardiac progenitor cells	10–50	$\sim 1\text{--}2$ <sup>18</sup>
Embryonic stem cells	8–20	$\sim 1\text{--}6$ <sup>19</sup>
Inducible pluripotent stem cells	10–50	$\sim 1$ <sup>20</sup>

indices (e.g., ejection fraction, ventricular volumes, etc.)<sup>1-3,16</sup>.

Overall, iPSCs<sup>13,14</sup> are more advantageous but still face critical challenges<sup>21</sup> that can be potentially addressed with next generation therapies, including polymeric biodegradable scaffolds and three-dimensional constructs. These constitute optimal test beds that can be used to mediate the proinflammatory/fibrotic/apoptotic responses, in combination with the use of cytokines, microribonucleic acid (miRNA), growth factors, noncoding RNA constructs, and extracellular vesicles, to achieve improved engraftment<sup>1,22</sup> and viability under hypoxic states, immunogenicity, electrical topology<sup>23</sup>, cellular differentiation<sup>24</sup>, and the elimination of arrhythmogenic events<sup>19</sup>.

Despite the preclinical and clinical findings, there are no known noninvasive techniques that allow cellular monitoring following SC therapy. In this sense, the lack of means is limiting. Accordingly, only external biomarkers are employed for functional evaluation and tissue characterization. Correspondingly, direct, noninvasive tracking of the SC would potentially allow monitoring of cellular engraftment and proliferation of therapy [as this pertains to the evolution of MI (Phases I–V)], and would thus serve as an essential tool for the assessment and potential quantification of myocardial recovery at the cellular/molecular levels.

## Noninvasive Magnetic Resonance Imaging and Tracking

The synthesis and identification of potential candidates for preclinical and clinical magnetic resonance imaging (MRI) and tracking of SCs have been based on (a) the assessment of SC efficacy, (b) monitoring of delivery, and (c) tracking of SC fate (engraftment and potential therapeutic outcomes)<sup>25</sup>. Accordingly, the chemical syntheses of these compounds aimed to achieve ideal cell label imaging characteristics, including (a) biocompatibility, (b) increased specificity to target cells, (c) increased MRI detection sensitivity (> a few thousands of cells/voxel), (d) minimal label dilution upon division, (e) lack of long-term toxicity, (f) capacity for direct quantification from images (in direct proportionality to cell number)<sup>26,27</sup>, and (g) minimal interference with other cellular functions and viability<sup>25,28,29</sup>. To-this-date, no probe has been identified that can fulfill all (or most) of these

requirements. Adopted labeling techniques have included (a) receptor-based, (b) reporter gene labeling, and (c) direct labeling approaches. The evolution of SC surface markers during their differentiation/division has limited the preclinical and clinical applicability of receptor-based labeling strategies. Direct labeling has thus dominated preclinical/clinical applications. This technique involves the *in vitro* coculture of the target label with cells (typically for a few hours) during which the label is either attached to the cell membrane or endocytosed. Transfection agents have been used to enhance the payload (protamine-sulfate<sup>30</sup>, lipofectamine<sup>31</sup>) but the label increases have been moderate.

<sup>1</sup>H- and <sup>19</sup>F-based label compounds have been developed for SC labeling and MR imaging and tracking. The former have included (a) iron oxides [monocrystalline paramagnetic iron oxide nanoparticles (MPIO-NPs)/Feridex, superparamagnetic iron oxide nanoparticles (SPIOs), and ultrasmall superparamagnetic iron oxide NPs], (b) gadolinium chelates, (c) microcapsules, and (d) reporter genes (enzyme-based or transporter-based)<sup>25</sup>. Owing to the increased gadolinium concentration requirements and safety concerns, and the large sizes of microcapsules (diameters in the range of 300–500  $\mu\text{m}$ ) (as noted previously<sup>25,32</sup>), iron oxides have been preferred for labeling. Successful cardiovascular imaging applications have been demonstrated in normal and infarcted animals and in humans. However, to-this-date, human applications have targeted organs other than the heart (and have involved melanoma<sup>33</sup>, head trauma<sup>34</sup>, spinal cord<sup>35</sup>, type I diabetes<sup>36</sup>, and multiple sclerosis/amyotrophic lateral sclerosis<sup>37</sup> patients). Additionally, multiple preclinical studies have been conducted since 2003 that have involved a range of cell types [MSCs<sup>38,39</sup>, ESCs<sup>40</sup>, bone-marrow SCs (BMSCs)<sup>41</sup>, and rat (R2.2) CPCs<sup>42</sup>], animals (mice<sup>40</sup>, rats<sup>41,42</sup>, dogs<sup>43</sup>, and pigs<sup>38,39,44</sup>), and field strengths ( $\geq 1.5$  T) with different iron oxide constructs (Ferumoxides<sup>44</sup>, SPIOs<sup>41</sup>, and MPIOs<sup>42</sup>).

Despite the advantages (lack of toxicity, safety, low-concentration requirements) and the successes of iron oxide particles for labeling, these efforts have been hampered by the (a) negative contrast (susceptibility-induced signal loss)<sup>32</sup>, (b) low sensitivity [compared with other imaging modalities, e.g., positron emission tomography (PET)/single-photon emission computed tomography]<sup>45</sup>, (c) inability to relate the signal loss with cell viability, (d) incompatible use in patients with pacemakers, (e) withdrawal of the Food and Drug Administration license for commercial use, and (f) cost. Nonetheless, the fundamental scientific limitations associated with these particles pertain to the regions with hypointense signals and the fact that these region(s) may or may not relate to labeled viable cells in that the label may concurrently coexist in apoptotic cells (in addition to viable SCs), in the extracellular space as free label following cell lysis, or in circulating macrophages that may reside on site. Notable is the fact that hypointense areas in normal or remote regions of the infarcted myocardium disappeared after 1 week<sup>39</sup>, while hypointense regions in infarcted areas persisted for multiple weeks

postinjection of iron oxide NPs. While the survival of SCs in MI regions may be more robust<sup>39</sup>, the exact mechanism, etiology for the observed hypointense regions, and the clearance kinetics for periods  $> 2$  weeks postinjection, remain largely unexplored. The findings attesting to the persistence of hypointense signals are corroborated primarily and foremost by the plausible hypothesis that the administered agent may persist in different forms (free, in necrotic/apoptotic cells, or in circulating macrophages), secondary to the unavailability of accessible vascular routes for clearance owing to microvascular obstruction.

Contrary to iron particles in <sup>1</sup>H MRI, fluorinated <sup>19</sup>F NP labels have been introduced as intravenous contrast agents as novel, highly sensitive, exogenously administered <sup>19</sup>F signal beacons (encapsulated by inert/biodegradable polymeric sheaths) given that MR-visible fluorine is absent from endogenous human tissues. The primary constructs include perfluorocarbon ether NPs (PFCE comprising 20 chemically equivalent fluorine atoms with diameters in the range of 85–200 nm<sup>26,46</sup> and perfluorooctyl bromide nanoemulsions (PFOB-NE comprising 17 fluorine atoms, diameters of approximately 210 nm<sup>47</sup>), yet newer clinically applicable constructs (ABL-101) have been reported recently<sup>48</sup>. Despite the relative merits and disadvantages of these label types (MR sensitivity, half-lives, clearance kinetics), they had been used originally in immune therapy<sup>33,49</sup>, and myocardial inflammation research studies (PFCE)<sup>50,51</sup> but found their ways in clinical trials in colorectal cancer treatments with immunotherapeutic dendritic cell vaccination (PFC)<sup>26</sup> and in inflammation in coronary artery disease (PFOB)<sup>47</sup>. They have been recently approved for another cell tracking/therapy clinical trial (PFCE) [ClinicalTrials.gov, Identifier: NCT02574377]. Their clinical efficacies and safety profiles have thus been proven/established.

The major MR benefits of these probes stem from their excellent positive contrast (in comparison with iron oxides), enhanced specificity, fast biodistribution (owing to their small sizes), and their capacities for direct clinical translatability. Nonetheless, the imaging technique is limited by the low-spatial resolution (compared with <sup>1</sup>H MRI) and lower sensitivity (compared with equivalent optical and PET imaging techniques). <sup>19</sup>F MRI has also been criticized<sup>52</sup> for its limiting technical requirements pertaining to dedicated hardware and software. Nevertheless, to my understanding, the latter are neither preclusive nor limiting for widespread preclinical/clinical use. Additionally, typical/conventional, commonly available pulse sequences may be used for imaging acquisitions<sup>53,54</sup>.

The major challenges associated with the use of these probes in SC imaging and tracking stem from the low intracellular concentrations achieved following labeling<sup>55</sup>, low signal-to-noise ratio (SNR) responses (especially at low/clinical field strengths at 1.5 and 3 T), the confounding effects of isoflurane anesthesia<sup>55</sup>, and the inability to detect them with conventional MR imaging acquisition protocols. Increasing the labeling dose is prohibitive to cellular

function and viability. Clinically approved transfection agents and/or electroporation yielded improved but did not substantially increase payloads<sup>56</sup>.

While fluorinated NPs had been used to label, image, and track SCs in stroke patients<sup>57</sup>, cardiac applications with SCs had been unsuccessful<sup>58,59</sup>. We managed to successfully increase the intracellular efficiency of <sup>19</sup>F labeling by four- to eight-fold in CPCs with FuGENE (corresponding <sup>19</sup>F MRI SNR increases in the order of 4.4–14 times *in vitro* compared with simple labeling) without any effects on viability<sup>56</sup>. These findings were corroborated by the four-fold fluorescent signal increases of FuGENE-labeled SCs compared with simply labeled cells with the same NPs (conjugated with Atto647) on the first day (D1) after labeling.

Based on these accomplishments, *in vivo* imaging and SC tracking was successfully achieved in mice at 9.4 T (detection of approximately 10 k cells per voxel<sup>53</sup>) with <sup>19</sup>F MRI/MRS<sup>56</sup> within a few minutes with conventional gradient echo pulse sequences<sup>53</sup>. More importantly, the protocol for cell preparation and injection has potential to be directly translatable to the clinic. Nevertheless, longitudinal studies demonstrated fluorine signal decreases up to ~31% at D7/D8 compared with evoked signals on D1 post-intramyocardial SC injection. *In vivo* findings were also consistent with *ex vivo* electron microscopy/optical fluorescence microscopy<sup>60</sup> studies that confirmed that the intracellular label signal from these cells dropped considerably within 2–4 days following labeling, primarily owing to fluorophore cleavage and intracellular NP processing (lysosomal destruction of endosomally packaged NPs and exocytosis) at a timescale faster than cell division (an effect that is expected to become more prominent in hypoxic states *in vivo*), and secondary to subsequent label dilution in proliferative or apoptotic states (at and following D3).

Several mechanisms may cause the temporally dependent signal attenuation observed in cardiac <sup>19</sup>F MRI *in vivo*. As discussed previously<sup>55</sup>, these may include (a) hypoxic-induced cell death, (b) macrophage infiltration and label scavenging, (c) limited SC proliferation and label dilution, (d) cell dispersion, migration, and either (i) lysis and label release in the extracellular space or (ii) SC migration into the circulatory system. While most of these hypotheses cannot be easily (and have not been) proven, we have provided preliminary immunostaining evidence attesting to the infiltration of macrophages at the injection site at D7/D8<sup>56</sup>. The temporal kinetics of monocyte infiltration and their persistence in remote and infarcted regions of the myocardium have been explored independently with direct intravenous infusions of PFCE NPs<sup>8,51</sup> preclinically (mouse), and with PFOB NPs (pig)<sup>50</sup> preclinically and clinically<sup>47</sup>. Most of these studies agree that a more complex monocyte phenotype—comprising classical and intermediate (inflammatory M1) and nonclassical (regenerative M2) monocytes—is involved/coexists in MI. Furthermore, the spatiotemporal dynamics of macrophage infiltration and

their persistence at the infarct zone have been detected as early as D3 post-MI, have been shown to peak at D7, and to persist for approximately 3 weeks in the murine heart<sup>51</sup>. Interestingly, <sup>19</sup>F signal changes in remote and infarct/peri-infarct zones yielded similar temporal patterns and trends (fluorine MR signals in MI were highly correlated with macrophage content)<sup>51</sup>, yet the <sup>19</sup>F signal intensities were by far greater in MI compared with remote zones. In contrast, no significant monocyte changes were observed in healthy, acute ST-elevation MI, and stable coronary artery disease patients with PFOB, albeit the reported temporally increasing monocytic trends in these groups for periods up to 6–7 days post-MI<sup>47</sup>.

In comparison with the adverse environment SCs experience following direct injections, scaffolds have provided an improved test bed for these cells that has facilitated proliferation and promoted improved engraftment<sup>22</sup>. With proper enrichments, scaffolds have the potential to induce angiogenesis, assist SC migration, trigger appropriate signaling pathways to prolong viable states, and achieve improved engraftment rates. Our recent efforts with biodegradable polyhydroxyalkanoate/polycaprolactone blend scaffolds seeded with CPCs<sup>61</sup> have prolonged the capacity to image and track the seeded cells *in vitro* from approximately 2–4 days (direct intramyocardial administration paradigm)<sup>53</sup> to >9 days. *In vivo* implantation of seeded scaffolds on the healthy murine epicardium yielded improved <sup>19</sup>F signal persistence at D7 compared with direct intramyocardial injections<sup>56</sup>. Accordingly, the useful temporal window for imaging and tracking has been extended considerably. Nevertheless, the major shortcomings of MRI contrast agents still relate to the potential mechanism of label dilution or degradation (within a timeframe of 3–4 days). Possible non-associative binding of released PFCE label on the scaffolds may also lead to the persistence of the <sup>19</sup>F MRI signal and to false indications on viable SC presence.

## Potential Value of <sup>19</sup>F MRI in Cardiovascular Regeneration in MI

Considerable advances have been documented since the introduction and use of SCs for cardiac regeneration. While the potential fate of SCs in cardiac regeneration is still unclear, robust preclinical and clinical cell labeling and tracking methods have been demonstrated in healthy and diseased cardiac tissue. The shortcomings of iron oxide agents have redirected research attention to <sup>19</sup>F NPs that possess unique positive contrast and increased MR sensitivity characteristics. We have successfully demonstrated fast, noninvasive MR imaging and tracking of CPCs in the healthy murine heart *in vivo* (a) directly (intramyocardial injections) and (b) with biodegradable polymeric scaffolds. The protocols are directly translatable to the clinic and unequivocally justify the potential value and significance of <sup>19</sup>F MRI in cardiovascular regeneration in disease. Nevertheless, the major challenges for widespread applicability

of these approaches pertain to (a) the prolongation of the useful imaging window (detectable  $^{19}\text{F}$  signal levels) beyond 8 days postcellular injection, (b) the determination of the sources of the  $^{19}\text{F}$  signal following transplantation (viable cell label, MR detectable signal from free label released from cells in processed or unprocessed forms, presence of MR-visible label that has been uptaken by circulating macrophages), (c) the identification of optimal signal sensitivity/detectability limits at clinical field strengths (3 T or 1.5 T), (d) conclusive identification/confirmation of the MR-visible signal sources on polymeric scaffolds (at the SC seeding or subsequent stages, e.g., following cell lysis), and (e) the identification on whether there are signal changes attributed to enhanced proliferation/engraftment in hypoxic states.

The inability of direct  $^{19}\text{F}$  labeling to achieve long-term SC tracking limits its range of applications. Nevertheless, the technique is highly beneficial and outperforms alternative methods in the assessment of the (a) temporal evolution of cardiac disease, including the acute phases of MI (Phases I–III) and (b) fast and temporally evolving inflammation (infarction, myocarditis, other). It is likely that clinically useful temporal imaging/tracking can be achieved within 1–2 weeks, especially in MI in which the SC responses (in hypoxic states) are more robust. Reinforcing these arguments, the role and applicability of  $^{19}\text{F}$  MRI and short-term SC tracking is expected to benefit (a) theranostic efforts for drug delivery and the evaluation of the therapeutic efficacy in the acute phases of MI, (b) the temporal evaluation of angiogenic responses (with and without the concurrent administration of growth factors), (c) the assessment of the efficacy of combined cell therapies (primary SCs mixed with immune cells), and (d) the evaluation of different test beds for SC therapy. Invariably,  $^{19}\text{F}$  MRI is expected to provide a unique biomarker signature and will serve as a key mediator for molecular intervention during the inflammatory and remodeling phases of cardiac disease (in conjunction with short-term SC tracking), while the role of  $^{19}\text{F}$  MRS in the identification of long-term SC tracking and viability assessment should not be underestimated.

In conclusion, it is believed that a clear potential exists for the clinical applicability of  $^{19}\text{F}$  MRI for short-term monitoring of labeled SCs in cardiovascular disease and in inflammation as it pertains to the assessment of routine therapeutic, theranostic, and transplantation interventions and outcomes. However, important scientific and technical challenges must be addressed and elucidated first—including the evaluation of the tracking limits of SC therapy in disease, the establishment of the technique's efficacy for theranostic and other drug applications, the technique's applicability for dual-cell therapeutic interventions, extensive evaluations of polymeric scaffold test beds, and the elucidation of the role of  $^{19}\text{F}$  MRS for assessing long-term SC viability—before the technique's endorsement in routine clinical practice is considered/realized.

## Acknowledgments

I am most grateful to Professors, colleagues, collaborators, staff, and students at the Departments of Cardiovascular Medicine and Physiology, Anatomy, and Genetics at the University of Oxford and at the Department of Life Sciences at the University Westminster, London, for their support, advice, and collaboration during the period of 2015–2017. I am particularly grateful to Professor M. Srinivas at the Radboud University Medical Center and her lab members for the support and productive collaborations during the past 5 years.


## Declaration of Conflicting Interests

The author(s) declared no potential conflicts of interest with respect to the research, authorship, and/or publication of this article.

## Funding

The author(s) received no financial support for the research, authorship, and/or publication of this article.

## ORCID iD

Christakis Constantinides  <https://orcid.org/0000-0001-9225-7572>

## References

1. Mehasche P, Vanneaux V, Hagege A, Bel A, Cholley B, Cacciapuoti I, Parouchev A, Benhamouda N, Tachdjian G, Tosca L, Trouvin J-H, et al. Human embryonic stem cell-derived cardiac progenitors for severe heart failure treatment: first clinical case report. *Eur Heart J*. 2015;36(30):2011–2017.
2. Nakamura K, Murry CE. Function follows form – A review of cardiac cell therapy. *Circ J*. 2019;83(12):2399–2412.
3. Lemcke H, Voronina N, Steinhoff G, David R. Recent progress in stem cell modification for cardiac regeneration. *Stem Cells Int*. 2018;2018:1909346.
4. Menasche P. Cell therapy trials for heart regeneration—lessons learned and future directions. *Nat Rev Cardiol*. 2018;15(11):659–671.
5. Bartunek J, Terzic A, Davison BA, Filippatos GS, Radovanovic S, Beleslin B, Merkely B, Musialek P, Wojakowski W, Andreaka P, Horvath IG, et al. Cardiopoietic cell therapy for advanced ischaemic heart failure: results at 39 weeks of the prospective, randomized, double blind, sham-controlled CHART-1 clinical trial. *Eur Heart J*. 2017;38(9):648–660.
6. Blankensteijn WM, Creemers E, Lutgens E, Cleutjens JP, Daemen MJ, Smits JF. Dynamics of cardiac wound healing following myocardial infarction: observations in genetically altered mice. *Acta Physiol Scand*. 2001;173(1):75–82.
7. Frangiannis NG. Pathophysiology of myocardial infarction. *Compr Physiol*. 2015;5(4):1841–1875.
8. Lanza GM. Dual-contrast  $^{19}\text{F}/^1\text{H}$  MRI to characterize myocardial infarct healing: advancing the horizon for MR microscopy with clinical MR scanners. *Circ Cardiovasc Imag*. 2018;11(11):e008457.
9. Serhan CN, Petasis NA. Resolvins and protectins in inflammation resolution. *Chem Rev*. 2011;111(10):5922–5943.
10. Serhan CN. Pro-resolving lipid mediators are leads for resolution physiology. *Nature*. 2014;510(7503):92–101.

11. Ogle ME, Segar CE, Sridhar S, Botchwey EA. Monocytes and macrophages in tissue repair: implications for immunoregenerative biomaterial design. *Exp Biol Med* (Maywood). 2016; 241(10):1084–1097.
12. Cambria E, Pasqualini FS, Wolint P, Gunter J, Steiger J, Bopp A, Hoerstrup SP, Emmert MY. Translational cardiac stem cell therapy: advancing from first-generation to next-generation cell types. *NPJ Regen Med*. 2017;2:17.
13. Eschenhagen T, Bolli R, Braun T, Field LJ, Fleischmann BK, Frisen J, Giacca M, Hare JM, Houser S, Lee RT, Marban E, et al. Cardiomyocyte regeneration: a consensus statement. *Circulation*. 2017;136(7):680–686.
14. Lopez E, Blaquez R, Marinaro F, Alvarez V, Blanco V, Baez C, Gonzalez I, Abad A, Moreno B, Margallo FMS, Crisostomo V, et al. The intrapericardial delivery of extracellular vesicles from cardiosphere-derived cells stimulates M2 polarization during the acute phase of porcine myocardial infarction. *Stem Cell Rev Rep*. 2019;16(3):612–625. doi:10.1007/s120150-019-09926-y.
15. Stevens KR, Murry CE. Human pluripotent stem cell-derived engineered tissues: clinical considerations. *Cell Stem Cell*. 2018;22(3):294–297.
16. Wang LL, Liu Y, Chung JJ, Wang T, Gaffey AC, Lu M, Cavanaugh CA, Zhou S, Kanade R, Aliuri P, Morrissey EE, et al. Local and sustained miRNA delivery from an injectable hydrogel promotes cardiomyocyte proliferation and functional regeneration after ischemic injury. *Nat Biomed Eng*. 2017;1:983–992.
17. Zhan XS, El-Ashram S, Luo DZ, Luo HN, Wang BY, Chen SF, Bai YS, Chen ZS, Liu CY, Ji HQ. A comparative study of biological characteristics and transcriptome profiles of mesenchymal stem cells from different canine tissues. *Int J Mol Sci*. 2019;20(6):1485.
18. Nakamura T, Hosoyama T, Kawamura D, Takeuchi Y, Tanaka Y, Samura M, Ueno K, Nishimoto A, Kurazumi H, Suzuki R, Ito H, et al. Influence of aging on the quantity and quality of human cardiac stem cells. *Sci Rep*. 2016;6:22781.
19. Cowan CA, Klimanskaya I, McMahon J, Atienza J, Witmyer J, Zucker JP, Wang S, Morton CC, McMahon AP, Powers D, Melton DA. Derivation of embryonic stem-cell lines from human blastocysts. *N Engl J Med*. 2004;350(13):1353–1356.
20. Chatterjee I, Li F, Kohler EE, Rehman J, Malik AB, Wary KK. Induced pluripotent stem (iPS) cell culture methods and induction of differentiation into endothelial cells. *Methods Mol Biol*. 2016;1357:311–327.
21. Bertero A, Murry CE. Hallmarks of cardiac regeneration. *Nat Rev Cardiol*. 2015;15(10):579–580.
22. Li X, Tamara K, Xie X, Guan J. Improving cell engraftment in cardiac stem cell therapy. *Stem Cells Int*. 2016;2016:7168797.
23. Shiba Y, Filice D, Fernandes S, Minami E, Dupras SK, va Biber B, Trinh P, Hirota Y, Gold JD, Viswanathan M, Laflamme MA. Electrical integration of human embryonic stem cell-derived cardiomyocytes in a guinea pig chronic infarct model. *J Cardiovasc Pharmacol Ther*. 2014;19(4):368–381.
24. Zhang J, Zhu W, Radisic M, Vunjak-Novakovic G. Can we engineer a human cardiac patch for therapy? *Circ Res*. 2018; 123(2):244–265.
25. Azene N, Fu Y, Maurer J, Kraitchman DL. Tracking of stem cells *in vivo* for cardiovascular applications. *J Cardiovasc Magn Reson*. 2014;16(1):7.
26. Srinivas M, Cruz LJ, Bonetto F, Heerschap A, Figdor CG, de Vries JM. Customizable, multi-function fluorocarbon nanoparticles for quantitative *in vitro* imaging using <sup>19</sup>F MRI and optical imaging. *Biomaterials*. 2010;31(27):7070–7077.
27. Srinivas M, Heerschap A, Ahrens ET, Figdor CG, de Vries IJM. <sup>19</sup>F MRI for quantitative *in vivo* cell tracking. *Trends Biotechnol*. 2010;28(7):363–370.
28. Fu Y, Azene N, Xu Y, Kraitchman DL. Tracking stem cells for cardiovascular applications *in vivo*: focus on imaging techniques. *Imaging Med*. 2011;3(4):473–486.
29. Ahrens ET, Helfer BM, O'Hanlon CF, Schirda C. Clinical cell therapy imaging using a perfluorocarbon tracer and fluorine-19 MRI. *Magn Reson Med*. 2014;72(6):1696–1701.
30. Arbab AS, Yocum GT, Kalish H, Jordan EK, Anderson SA, Khakoo AY, Read EJ, Frank JA. Efficient magnetic cell labeling with protamine sulfate complexed to ferumoxides for cellular MRI. *Blood*. 2004;104(4):1217–1223.
31. Toyoda K, Tooyama I, Kato M, Sato H, Morikawa S, Hisa Y, Inubushi T. Effective magnetic labeling of transplanted cells with HVJ-e for magnetic resonance imaging. *Neuroreport*. 2004;15(4):589–593.
32. Zhang WY, Ebert AD, Narula J, Wu JC. Imaging cardiac stem cell therapy: translations to human clinical studies. *J Cardiovasc Transl Res*. 2011;4(4):514–522.
33. deVries IJ, Lesterhuis WJ, Barentsz JO, Verdijk P, van Krieken JH, Boerman OC, Oyer WJG, Bonenkamp JJ, Boezeman JB, Adema GJ, Bulte JWM, et al. Magnetic resonance tracking of dendritic cells in melanoma patients for monitoring of cellular therapy. *Nat Biotechnol*. 2005;23(11):1407–1413.
34. Zhu J, Zhou L, Zing Wu F. Tracking neural stem cells in patients with brain trauma. *N Engl J Med*. 2006;355(22): 2376–2378.
35. Callera F, de Melo CM. Magnetic resonance tracking of magnetically labeled autologous bone marrow CD34+ cells transplanted into the spinal cord via lumbar puncture technique in patients with chronic spinal cord injury: CD34+ cells' migration into the injured site. *Stem Cells Dev*. 2007;16(3):461–466.
36. Toso C, Vallee JP, Morel P, Ris F, Demuylder-Mischler S, Lepetit-Coiffe M, Marangon N, Saudek F, Shapiro AMJ, Bosco D, Berney T. Clinical magnetic resonance imaging of pancreatic islet grafts after iron nanoparticle labeling. *Am J Transplant*. 2008;8(3):701–706.
37. Karussis D, Karageorgiou C, Vaknin-Dembinsky A, Gowda-Kurkalli B, Gomori JM, Kassis I, Bulte JW, Petrou P, Ben-Hur T, Abramsky O, Slavin S. Safety and immunological effects of mesenchymal stem cell transplantation patients with multiple sclerosis and amyotrophic lateral sclerosis. *Arch Neurol*. 2010; 67(10):1187–1194.
38. Hill JM, Dick AJ, Raman VK, Thompson R, Yu ZX, Hinds KA, Pessanha BS, Guttman MA, Varney TR, Martin BJ, Dunbar CE, et al. Serial cardiac magnetic resonance imaging of injected mesenchymal stem cells. *Circulation*. 2003;108(8): 2009–2014.

39. Kraitchman DL, Helman AW, Atalar E, Amado LC, Martin BJ, Pittenger MF, Hare JM, Bulte JW. *In vivo* magnetic resonance imaging of mesenchymal stem cells in myocardial infarction. *Circulation*. 2003;107(18):2290–2293.
40. Ebert SN, Taylor DG, Nguyen HL, Bevers RJ, Xu Y, Yang Z, French BA. Noninvasive tracking of cardiac embryonic stem cells *in vivo* using magnetic resonance imaging techniques. *Stem Cells* 2007;25(11):2936–2944.
41. Stuckey DJ, Carr CA, Martin-Renton E, Tyler DJ, Willmott C, Cassidy PJ, Hale SJ, Schneider JE, Tatton L, Harding SE, Radda GK, et al. Iron particles for noninvasive monitoring of bone marrow stromal cell engraftment into, and isolation of viable engrafted donor cells from, the heart. *Stem Cells*. 2006; 24(8):1968–1975.
42. Carr CA, Stuckey DJ, Tan JJ, Tan SC, Gomes RS, Camelliti P, Messina E, Giacomello A, Ellison GM, Clarke CK. Cardiosphere-derived cells improve function in the infarcted rat heart for at least 16 weeks—an MRI study. *PLoS One*. 2011; 6(10):e25669.
43. Soto AV, Gilson WD, Kedziorek D, Fritzsche D, Izbudak I, Young RG, Pittenger MF, Bulte JW, Kraitchman DL. MRI tracking of regional persistence of feridex-labeled mesenchymal stem cells in a canine myocardial infarction model. *J Cardiovasc Magn Reson*. 2006;8:89–90.
44. Amado LC, Saliaris AP, Schuleri KH, John MS, Xie J-S, Cattaneo S, Durand DJ, Fitton T, Kuang JQ, Stewart G, Lehrke S, et al. Cardiac repair with intramyocardial injection of allogeneic mesenchymal stem cells after myocardial infarction. *Proc Natl Acad Sci U S A*. 2005;102(32):11474–11479.
45. Pearl J, Wu JC. Seeing is believing: tracking cells to determine the effects of cell transplantation. *Thorac Cardiovasc Surg*. 2008;20(2):102–109.
46. Swider E, Stall AHJ, van Riessen K, Jacobs L, White PB, Fokkink R, Janssen H-J, van Dinther E, Figdor CG, de Vries JM, Koshkina O, et al. Design of triphasic poly(lactic-co-glycolic acid) nanoparticles containing a perfluorocarbon phase for biomedical applications. *RSC Adv*. 2018;8(12): 6460–6470.
47. Nienhaus F, Colley D, Jahn A, Pfeiler S, Flocke V, Temme S, Kelm M, Gerdes N, Bonner F. Phagocytosis of a PFOB-nanoemulsion for <sup>19</sup>F magnetic resonance imaging: first results in monocytes of patients with stable coronary artery disease and ST-Elevation myocardial infarction. *Molecules*. 2019;24(11):2058.
48. Darcot E, Colotti R, Brennan D, Deuchar GA, Santosh C, van Heeswijk RB. A characterization of ABL-101 as a potential tracer for clinical fluorine-19 MRI. *NMR Biomed*. 2019; 33(11):e4212.
49. Bonetto F, Srinivas M, Heerschap A, Mailliard R, Ahrens ET, Figdor CG, de Vries IJM. A novel <sup>19</sup>F agent for detection and quantification of human dendritic cells using magnetic resonance imaging. *Int J Cancer*. 2010;129(2):365–373.
50. Bonner F, Merx MW, Klingel K, Begovatz P, Fogel U, Sager M, Temme S, Jacoby C, Ravesh MS, Grapentin C, Schubert R, et al. Monocyte imaging after myocardial infarction with <sup>19</sup>F MRI at 3 T T: a pilot study in explanted porcine hearts. *Eur Heart J Cardiovasc Imaging*. 2015;16(6):612–620.
51. Ramos IT, Henningson M, Nezafat M, Lavin B, Lorrio S, Gebhardt P, Protti A, Eykyn TR, Andia ME, Fogel U, Phinikaridou A, et al. Simultaneous assessment of cardiac inflammation and extracellular matrix remodeling after cardiovascular infarction. *Circ Cardiovasc Imaging*. 2018;11(11):e007453.
52. Fu U, Kraitchman DL. Stem cell labeling for noninvasive delivery and tracking in cardiovascular regenerative therapy. *Expert Rev Cardiovasc Ther*. 2010;8(8):1149–1160.
53. Constantinides C, Maguire M, McNeill E, Carnicer R, Swider E, Srinivas M, Carr CA, Schneider JE. Fast, quantitative, murine cardiac <sup>19</sup>F MRI/MRS of PFCE-labeled progenitor stem cells and macrophages at 9.4 T. *PLoS One*. 2018;13(1): e0190558.
54. van Heeswijk RB, Blois J, Kania G, Gonzales C, Blyszczuk P, Stuber M, Erriksson U, Schwitter J. Selective *in vivo* visualization of immune-cell infiltration in a mouse model of autoimmune myocarditis by fluorine-19 cardiac magnetic resonance. *Circ Cardiovasc Imaging*. 2013;6(2):277–284.
55. Constantinides C, Maguire ML, Stork L, Swider E, Srinivas M, Carr CA, Schneider JS. Temporal accumulation and localization of isoflurane in the C57BL/6 mouse and assessment of its potential contamination in <sup>19</sup>F MRI with perfluoro-crown-ether-labeled cardiac progenitor cells at 9.4 Tesla. *J Magn Reson Imaging*. 2017;45(6):1659–1667.
56. Constantinides C, McNeill E, Carnicer R, Zen AAH, Sainz-Urruela R, Shaw A, Patel J, Swider E, Azalioan R, Potamiti L, Hadjisavvas A, et al. Improved cellular uptake of perfluorocarbon nanoparticles for *in vivo* murine cardiac <sup>19</sup>F MRS/MRI and temporal tracking of progenitor cells. *Nanomedicine*. 2019;18:391–401.
57. Boehm-Sturm P, Mengler L, Wecker S, Hoehn M, Kallur T. *In vivo* tracking of human neural stem cells with <sup>19</sup>F Magnetic Resonance Imaging. *PLoS One*. 2011;6(12):e29040.
58. Gomes RSM, Pires das Neves R, Cochlin L, Lima A, Carvalho R, Korpisaloo P, Dragneva G, Turunen M, Liimatainen T, Clarke K, Ylä-Herttua S, et al. Efficient pro-survival/angiogenic miRNA delivery by an MRI-detectable nanomaterial. *ACS Nano*. 2013;7(4):3362–3372.
59. Aday S, Paiva J, Sousa S, Gomes RSM, Pedreiro S, So P-W, Carr CA, Cochlin L, Gomes AC, Paiva A, Ferreira L. Inflammatory modulation of stem cells by Magnetic Resonance Imaging (MRI)-detectable nanoparticles. *RSC Adv*. 2014;60: 31706–31709.
60. Constantinides C, Potamiti L, Patsali P, Carr CA, Srinivas M, Hadjisavvas A, Kyriacou K. Intracellular uptake, localization, and excretion kinetics of PCFE nanoparticles used for cardiac stem cell labeling. *ESMI, Thessaloniki, Greece (virtual conference)*; March 2020.
61. Constantinides C, Basnett P, Lukasiewicz B, Carnicer R, Swider E, Majid QA, Srinivas M, Carr CA, Roy I. *In vivo* tracking and <sup>1</sup>H/<sup>19</sup>F magnetic resonance imaging of biodegradable polyhydroxyalkanoate/polyprolactone blend scaffolds seeded with labeled cardiac stem cells. *ACS Appl Mater Interf*. 2018;10(30):25056–25068.